# A Triethylenetetramine Bearing Anthracene and Benzophenone as a Fluorescent Molecular Logic Gate with Either−Or Switchable Dual Logic Functions

**Go Nishimura, Katsutake Ishizumi, Yasuhiro Shiraishi,* and Takayuki Hirai**

*Research Center for Solar Energy Chemistry and Division of Chemical Engineering, Graduate School of Engineering Science, Osaka University, Toyonaka 560-8531, Japan*

*Received: July 1, 2006; In Final Form: August 26, 2006*

Fluorescence behaviors of a triethylenetetramine bearing anthracene (AN) and benzophenone (BP) fragments at the respective ends, **L1**, have been studied in water, where effects of pH ($H^+$) and metal cations on the emission properties have been studied in detail. **L1** behaves as a fluorescent molecular logic gate driven by $H^+$ ($Input_1$) and metal cations ($Input_2$) as input chemicals. The most notable feature of **L1** is that this molecule expresses the "either−or" switchable dual logic functions. Operation of **L1** with $Cu^{2+}$ as $Input_2$ expresses the INHIBIT logic function, where a strong AN fluorescence appears only at pH 4 (with $H^+$) without $Cu^{2+}$ [$Input_1(1)$-$Input_2(0)$]. In contrast, operations of **L1** with all other metal cations as $Input_2$ express the TRANSFER logic function, where the presence of $H^+$ allows strong AN fluorescence regardless of whether the metal cation exists or not [$Input_1(1)$-$Input_2(0)$; $Input_1(1)$-$Input_2(1)$]. These emission switching behaviors of **L1** are driven by the difference in the coordination stability between **L1** and metal cations and the photoinduced intramolecular electron and energy transfer processes: (i) a pH-induced electron transfer from unprotonated nitrogen atoms of the polyamine chain to the photoexcited AN [ELT(N→AN*)]; (ii) a pH- and metal coordination-induced electron transfer from the photoexcited AN to the ground-state BP [ELT(AN*→BP)]; and (iii) a $Cu^{2+}$ coordination-induced energy transfer from the photoexcited AN to $Cu^{2+}$ [ENT(AN*→$Cu^{2+}$)].

## 1. Introduction

Design and development of fluorescent supramolecular systems, whose emission properties can be modulated by external inputs, is an area of intense research activity.[1] In particular, design of the systems performing elementary acts as electronic devices is of tremendous significance to the development of the miniaturized device components. Considerable efforts in this research area are motivated by a desire to develop future application of these components in a chemical computer.[2] Among the research, molecular systems capable of performing as a semiconductor logic gate have attracted a great deal of attention;[3] in particular, systems consisting of chemically encoded information as input and a fluorescent signal as output have been studied extensively. In these systems, the molecule demonstrates "on" or "off" switching of the fluorescence signal meaning "1" or "0" output, in response to the addition "1" or nonaddition "0" of the input chemicals. So far, various molecular systems expressing AND,[4] OR,[5] NOR,[6] INHIBIT,[7] XOR,[8] YES,[9] NOT,[10] and XNOR[11] logic functions have been proposed. However, most of the molecular systems express a single logic function by a combination of a certain two chemical inputs. Recent interest is focused on a molecule capable of demonstrating multiple logic functions by varying the input chemicals, in other words, a molecule whose logic functions can be *reconfigured* multiply by varying the input chemicals has attracted a great deal of attention (i.e., reconfigurable molecular logic gate).[12] Metal cations are often used as the input chemicals for reconfiguration of the logic functions,[12b,c] because the emission behavior of the fluorophores usually depends strongly on the nature of metal cations. This, however, also means that operations by different metal cation inputs inevitably express different logic functions;[12b] in other words, a certain logic function can only be expressed by a certain metal cation. A widely applicable fluorescent molecular logic gate must therefore combine (i) *reconfigurability* (expression of different logic functions by different metal cations) and (ii) *versatility* (expression of the same logic function by different metal cations). Such molecular systems, however, have not been proposed until now.

Earlier, we have reported pH-dependent fluorescence behaviors of a triethylenetetramine bearing anthracene (AN) and benzophenone (BP) fragments at the respective ends (**L1**) in water.[13] The AN fluorescence of **L1** is quenched weakly at pH 2−5 by an electron transfer from the photoexcited AN to the ground-state BP [ELT(AN*→BP)]. This occurs via an access of the AN and BP fragments by a pH-induced bending movement of the polyamine chain. In contrast, at pH >5, the AN fluorescence is strongly quenched by an electron transfer from the unprotonated nitrogen atoms of the polyamine chain to the photoexcited AN [ELT(N→AN*)], which is triggered by a pH-induced deprotonation of the nitrogen atoms of the polyamine chain.

In the present work, the effect of metal cations on the emission behavior of **L1** in water has been studied. We found that this simple-structured molecule **L1** acts as a fluorescent molecular logic gate operated by two chemical inputs, $H^+$ ($Input_1$) and metal cations ($Input_2$). We emphasize that this molecule behaves as the first fluorescent molecular logic system that combines reconfigurability and versatility: **L1** shows fluorescent outputs expressing the INHIBIT logic function by an operation with $Cu^{2+}$ as $Input_2$, while operations with all other metal cations as $Input_2$ express the TRANSFER logic function. We describe here that these emission switching behaviors of **L1** are driven by differences in the coordination stability

* To whom correspondence should be addressed. Phone: +81-6-6850-6271. Fax: +81-6-6850-6273. E-mail: shiraish@cheng.es.osaka-u.ac.jp.

10.1021/jp064131j CCC: $33.50 
Published on Web 10/06/2006

**SCHEME 1: Syntheses of L1 and L2**[a]

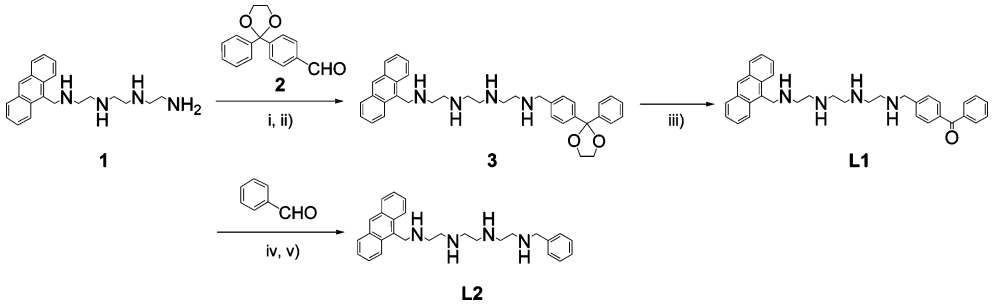


[a] Reagents and conditions: (i) **1**, **2**, ethanol, room temperature; (ii) $NaBH_4$, ethanol, 323 K; (iii) $HClO_4$, $CH_2Cl_2$, 273 K; (iv) **1**, benzaldehyde, ethanol, room temperature; (v) $NaBH_4$, ethanol, 323 K.

between **L1** and metal cations and the photoinduced intramolecular electron and energy transfer processes: (i) a pH-induced electron transfer from unprotonated nitrogen atoms of the polyamine chain to the photoexcited AN [ELT(N→AN*)]; (ii) an electron transfer from the photoexcited AN to the ground-state BP [ELT(AN*→BP)], which is driven by pH- and metal coordination-induced bending of the polyamine chain bringing the AN and BP fragments closer; and (iii) a $Cu^{2+}$ coordination-induced energy transfer from the photoexcited AN to $Cu^{2+}$ [ENT(AN*→$Cu^{2+}$)].

## 2. Experimental Section

**2.1. General.** All of the reagents used were of the highest commercial quality, which were supplied from Wako Pure Chemical Industries, Ltd. and Tokyo Kasei Co., Ltd. and used without further purification. Water was purified by the Milli Q system. **L1** and the reference compound, **L2**, a triethylenetetramine bearing AN and benzene moieties, were synthesized according to procedures summarized in Scheme 1 and as follows:[13]

*N*-{*2*-[(*Anthracene-9-ylmethyl*)*amino*]*ethyl*}-*N*′-{*2*-[(*benzophenone-4-ylmethyl*)*amino*]*ethyl*}-*ethane-1,2-diamine*, ***L1***. **1**[12b,14] (0.77 g, 2.3 mmol) and **2**[15] (0.56 g, 1.2 mmol) were dissolved in dry ethanol (50 mL) and the mixture was stirred at room temperature for 36 h under dry $N_2$. $NaBH_4$ (0.57 g, 15 mmol) was carefully added to the solution and was stirred at 323 K for 6 h. The solvent was removed by evaporation. Water (40 mL) and $CH_2Cl_2$ (90 mL) were added to the residue, and the resulting organic layer was dried over $Na_2SO_4$ and concentrated by evaporation, affording a yellow-white powder of **3** (0.45 g, yield: 72%). The **3** obtained (0.4 g, 0.63 mmol) was dissolved in ethanol, to which concentrated aqueous HCl solution was added slowly. The formed yellowish precipitate was recovered by filtration and dried in vacuo at 333 K, yielding **3**·4HCl (0.24 g, yield: 45%). $HClO_4$ (65% aqueous solution; 3 mL) was added slowly to a solution of **3**·4HCl (0.2 g, 0.32 mmol) dissolved in $CH_2Cl_2$ (30 mL) at 273 K, and the solution was stirred at 273 K for 1 h and at room temperature for 2 h. The solution was mixed with an aqueous $Na_2CO_3$ (2 g) solution (40 mL). The resulting organic layer was washed with water, dried over $Na_2SO_4$, and concentrated by evaporation. The resulting semisolid residue was dissolved in ethanol and precipitated by an addition of concentrated aqueous HCl solution, affording **L1**·4HCl (0.01 g, yield: 6.4%). $^1$H NMR (270 MHz, $D_2O$, TMS) $\delta$ (ppm) 3.24−3.61 (m, 12H, C$H_2$ of triethylenetetramine), 4.36 (d, 2H, ArC$H_2$), 5.30 (s, 2H, ArC$H_2$), 7.47−8.64 (m, 18H, Ar*H*); $^{13}$C NMR (270 MHz, $D_2O$, TMS) $\delta$ (ppm) 195.1, 135.6, 131.8, 131.7, 131.3, 131.1, 130.6, 130.4, 129.4, 128.8, 126.5, 52.3, 44.6, 44.4; FAB mass spectrum, *m*/*e* 531.3 (M + $H^+$). Anal. Calcd for $C_{35}H_{38}N_4O$·4HCl: C, 62.14; H, 6.26; N, 8.28. Found: C, 61.65; H, 6.51; N, 7.31. *N*-{*2*-[(*Anthracene-9-ylmethyl*)*amino*]*ethyl*}-*N*′-{*2*-[(*benzene-1-ylmethyl*)*amino*]*ethyl*}-*ethane-1,2-diamine*, ***L2.*** This material was synthesized in a manner similar to the synthesis of **L1** by reaction of **1** (0.50 g, 1.5 mmol) with benzaldehyde (0.16 g, 1.5 mmol), affording a yellow powder of **L2**·4HCl (0.58 g, yield: 68%). $^1$H NMR (270 MHz, $D_2O$, TMS) $\delta$ (ppm) 3.42−3.69 (m, 12H, C$H_2$ of triethylenetetramine), 4.34 (d, 2H, ArC$H_2$), 5.21 (s, 2H, ArC$H_2$), 7.49−8.57 (m, 14H, Ar*H*); $^{13}$C NMR (270 MHz, $D_2O$, TMS) $\delta$ (ppm) 134.5, 131.6, 131.2, 131.0, 130.6, 130.3, 129.4, 128.8, 126.4, 123.3, 52.0, 44.6, 44.5, 43.8; FAB mass spectrum, *m*/*e* 427.4 (M + $H^+$). Anal. Calcd for $C_{28}H_{34}N_4$·4HCl: C, 58.75; H, 6.69; N, 9.79. Found: C, 57.62; H, 7.11; N, 10.71.

**TABLE 1: The Stepwise Protonation Constants for L1**[a]

| reaction[b] | **L1** |
|---|---|
| H + L = HL | 8.53 ± 0.03 |
| H + HL = $H_2$L | 7.12 ± 0.06 |
| H + $H_2$L = $H_3$L | 5.01 ± 0.10 |
| H + $H_3$L = $H_4$L | 3.12 ± 0.24 |
| log $\beta$ | 23.79 |

[a] Determined in aqueous NaCl (0.15 M) solution at 298 ± 0.1 K. [b] Charges are omitted for clarity.

**2.2. Analyses.** Steady-state fluorescence spectra were measured on a Hitachi F-4500 fluorescence spectrophotometer (excitation and emission slit width, 2.5 nm). Absorption spectra were measured on an UV−visible photodiode-array spectrophotometer (Shimadzu; Multispec-1500). These spectra were measured at 298 ± 1 K, using a 10 mm path length quartz cell. All of the measurements were carried out in the presence of NaCl or $NaClO_4$ to maintain the ionic strength of the solution ($I$ = 0.15 M). For reproduction of the data, all of the spectral measurements were carried out in an aerated condition. Potentiometric titrations were carried out on a COMTITE-550 potentiometric automatic titrator (Hiranuma Co., Ltd.) with a glass electrode GE-101. Aqueous test solutions (50−60 mL) containing compounds (0.006−0.01 mmol) were kept under dry argon in the absence and presence of metal cations (1 equiv of the compound) with an ionic strength of $I$ = 0.15 M (NaCl or $NaClO_4$). The titrations were done at 298 ± 0.1 K, using an aqueous NaOH solution (0.35 M) as a base, and at least two independent titrations were performed. The protonation and intrinsic complexation constants of **L1** were determined by means of the nonlinear least-squares program HYPERQUAD, where the $K_w$ (=[$H^+$][$OH^-$]) value used was $10^{-13.73}$ (at 298 K).[16] The obtained stepwise protonation constants for **L1** and stability constants for interaction between **L1** and metal cations are summarized in Tables1 and 2, respectively. $^1$H NMR spectra were obtained by a JEOL JNM-GSX270 Excalibur, using TMS as standard. Semiempirical MO calculations were performed

**TABLE 2: The Stability Constants for Interaction between L1 and Metal Cations**[a]

| reaction[b] | $Cu^{2+}$ | $Zn^{2+}$ |
|---|---|---|
| M + **L1** = M**L1** | 14.39 ± 0.22 | 7.03 ± 0.05 |
| M**L1** + H = HM**L1** | 6.19 ± 0.43 | 7.36 ± 0.10 |
| H**L1** + M = HM**L1** | 12.06 ± 0.25 | 5.86 ± 0.07 |
| M**L1** + OH = M**L1**(OH) | 4.21 ± 0.38 | 5.23 ± 0.14 |
| M + **L1** + $H_2O$ = M**L1**(OH) + H | 4.87 ± 0.38 | −1.47 ± 0.08 |

[a] Determined in aqueous NaCl or $NaClO_4$ (0.15 M) solution at 298 K ± 0.1 K. [b] Charges are omitted for clarity.

with MNDO-*d* method within the WinMOPAC version 3.0 software (Fujitsu Inc.).[17]

## 3. Results and Discussion

**3.1. Effect of pH.** The effect of pH on the fluorescence behavior of **L1** has been described in a previous paper;[13] hence, only a brief description is made here. Figure 1A.i shows a pH-dependent change in fluorescence spectra of **L1** measured in water ($\lambda_{ex}$ = 368 nm). **L1** shows a distinctive fluorescence at 380−540 nm, assigned to an emission from the photoexcited AN fragment. The **L2** molecule bearing AN and benzene fragments (Scheme 1) shows emission spectra similar to that of **L1** (see the Supporting Information, Figure S1). Figure 1A.ii plots the fluorescence intensity of **L1** (open symbols) and **L2** (closed symbols) monitored at 416 nm against pH, where dotted lines in the figure denote the mole fraction distribution of the different **L1** species, which is calculated from the protonation constants determined potentiometrically (Table 1). **L2** shows almost the same distribution of the species as that of **L1**.[13] As shown by closed symbols in Figure 1A.ii, **L2** shows a strong AN fluorescence at acidic pH, whose intensity is almost constant at pH 2−5, but the intensity decreases with a pH increase, thus demonstrating a sigmoidal curve ($pK_a'$ = 6.7). The pH−fluorescence intensity profile of **L2** is explained by the protonation states of the nitrogen atoms within the polyamine chain: At pH 2−5, fully protonated $H_4$**L2**$^{4+}$ and the monodeprotonated $H_3$**L2**$^{3+}$ species exist predominantly. At pH >5, deprotonation of the $H_3$**L2**$^{3+}$ species produces the $H_2$**L2**$^{2+}$ species. This triggers an electron transfer from the unprotonated nitrogen atoms to the photoexcited AN fragment [ELT(N→AN*) process],[13,18] where 34% of the emission is quenched at pH 6 (79% $H_2$**L2**$^{2+}$ exists) based on the intensity obtained at pH 1.4 (>95% $H_4$**L2**$^{4+}$ exists). Further deprotonation leads to a further decrease in the fluorescence intensity, and total emission quenching takes place upon deprotonation of H**L2**$^{+}$ species.

As shown by open symbols in Figure 1A.ii, the pH−fluorescence intensity profile of **L1** does not show a sigmoidal curve: the intensity decreases gently with a pH increase over the pH 2−8 range. The fluorescence intensity of **L1** obtained at pH 4 is 49% lower than that obtained at pH 1.6. At pH 4, monodeprotonated $H_3$**L1**$^{3+}$ species exist predominantly (81%), while at pH 1.6, it is almost all fully protonated $H_4$**L1**$^{4+}$ species (>95%). The decrease in the fluorescence intensity, associated with a formation of $H_3$**L1**$^{3+}$ species, is due to an electron transfer from the photoexcited AN fragment to the ground-state BP [ELT(AN*→BP)]. This is triggered by a deprotonation of the polyamine chain, leading to an electrostatic repulsion of the chain.[18b] This brings the AN and BP fragments closer and, hence, triggers the ELT(AN*→BP) process ($\Delta G_{ELT(AN^*\rightarrow BP)}$ = −0.36 eV), thus resulting in the fluorescence intensity decrease.[13] Figure 2A.i shows the change in absorption spectra of **L1** with pH: absorption of **L1** red-shifts with a pH increase. This is because of a dipole−dipole interaction between the AN and BP fragments, indicating that pH increase actually brings these moieties closer.[19] In contrast, at pH >5, the ELT(N→AN*) process contributes mainly to the decrease in the fluorescence intensity (Figure 1A.ii), where $H_2$**L1**$^{2+}$, H**L1**$^{+}$, and **L1** species exist predominantly. Nanosecond time-resolved fluorescence decay measurements reveal that contribution of the rate constants, $k_{ELT(AN^*\rightarrow BP)}$ and $k_{ELT(N\rightarrow AN^*)}$ due to the ELT(AN*→BP) and ELT(N→AN*) quenching processes, to the overall fluorescence decay rate for the respective **L1** species, $k_{overall}$ (=$1/\tau_N + k_{ELT(AN^*\rightarrow BP)} + k_{ELT(N\rightarrow AN^*)}$),[20] is determined to be the following: 75% and 0% ($H_3$**L1**$^{3+}$), 6% and 15% ($H_2$**L1**$^{2+}$), 2% and 66% (H**L1**$^{+}$), and 1% and 84% (**L1**), respectively.[13] The results indicate that (i) the first deprotonation of the polyamine chain of **L1** ($H_3$**L1**$^{3+}$ species formation) triggers the ELT(AN*→BP) quenching process and (ii) the second (and later) deprotonation of **L1** triggers the ELT(N→AN*) quenching process.

As shown in Figure 3, the above emission behaviors of **L1** can be summarized as a logic operation. Operation of **L1** at pH 4 without metal cations [$Input_1$(1)-$Input_2$(0)] results in a strong AN fluorescence (Output = 1), although the ELT(AN*→BP) quenching process takes place (Figure 3A,B). In contrast, operation of **L1** at pH 8 without metal cations [$Input_1$(0)-$Input_2$(0)] shows very low fluorescence intensity (Output = 0), where the ELT(N→AN*) process strongly quenches the AN fluorescence (Figure 3A,B).

**3.2. Effect of $Cu^{2+}$ (Expression of the INHIBIT Logic Function).** As shown in Figure 3A,B, addition of $Cu^{2+}$ at both pH 4 and 8 [$Input_1$(1)-$Input_2$(1); $Input_1$(0)-$Input_2$(1)] leads to complete quenching of the **L1** fluorescence, resulting in 0 Outputs. Figure 1B.i shows the pH-dependent change in the fluorescence spectra of **L1** obtained with 1 equiv of $Cu^{2+}$. Figure 1B.ii plots the fluorescence intensity of **L1** (open symbols) against pH, where dotted lines in the figure denote mole fraction distribution of the different **L1** species, which is calculated from the protonation and stability constants determined potentiometrically (Tables 1 and 2). With $Cu^{2+}$, a decrease in the fluorescence intensity takes place at acidic pH in comparison to the intensity obtained without $Cu^{2+}$ (Figure 1A.ii, open symbols). Comparison of the pH−intensity profile with the distribution of the species reveals that the intensity decrease of **L1** occurs in conjunction with a $Cu^{2+}$−**L1** complex formation and becomes almost zero at pH >4, where metal-free **L1** species do not exit. A possible fluorescence quenching mechanism of **L1** with $Cu^{2+}$ is as follow: (i) an ELT(AN*→BP) process occurring between the AN and BP fragments, which are situated closely via the bending of the polyamine chain by the $Cu^{2+}$ coordination, and (ii) an energy transfer process from the photoexcited AN to a low-lying empty d-orbital of the coordinated $Cu^{2+}$ [ENT(AN*→$Cu^{2+}$)].[12d,21] As shown in Figure 1B.ii (closed symbols), use of **L2** shows a pH−fluorescence intensity profile similar to that of **L1**. Within **L2**, the ELT(benzene→AN* or AN*→benzene) processes do not occur because these processes are not favored thermodynamically.[13,19] These imply that the ENT(AN*→$Cu^{2+}$) process may be the main factor for the decrease in fluorescence intensity of **L1**. Figure 4 shows the change in the fluorescence intensity of **L1** at pH 4 as a function of $Cu^{2+}$ amount added. The **L1** fluorescence intensity decreases linearly with an increase in the $Cu^{2+}$ amount, and the complete quenching occurs upon addition of 1 equiv of $Cu^{2+}$ to **L1**. As shown in Figure 2B.i, $Cu^{2+}$ addition does not lead to any change in the absorption spectra of **L1** over the entire pH range, whereas the absence of $Cu^{2+}$ shows red-shifted absorption (Figure 2A.i) due to the dipole−dipole interaction between the

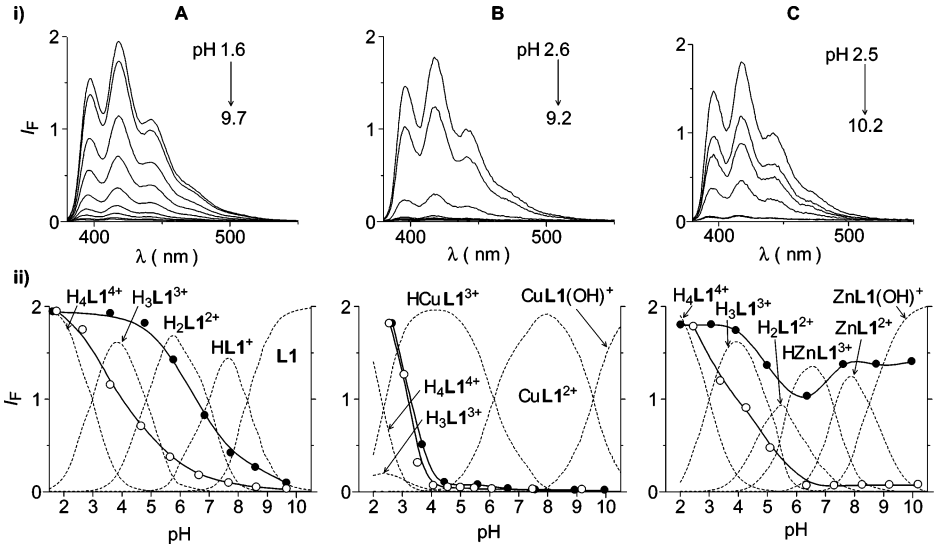


**Figure 1.** pH-dependent change in (i) fluorescence spectra ($\lambda_{ex}$ = 368 nm; 298 K) of **L1** and (ii) fluorescence intensity (monitored at 416 nm) of **L1** (open symbols) and **L2** (closed symbols) measured in the (A) absence and presence of (B) 1 equiv of $Cu^{2+}$ and (C) 1 equiv of $Zn^{2+}$ in aqueous NaCl or $NaClO_4$ (0.15 M) solution. The dotted lines in part ii denote mole fraction distribution of the different **L1** species. Each spectrum in part i corresponds to the plots in part ii [pH: (A) 1.6, 2.7, 3.6, 4.7, 5.7, 6.7, 7.7, 8.6, 9.7; (B) 2.6, 3.1, 3.5, 4.1, 4.6, 5.0, 5.5, 6.1, 7.5, 9.2; (C) 2.5, 3.4, 4.3, 5.1, 6.4, 7.3, 8.3, 9.2, 10.2].

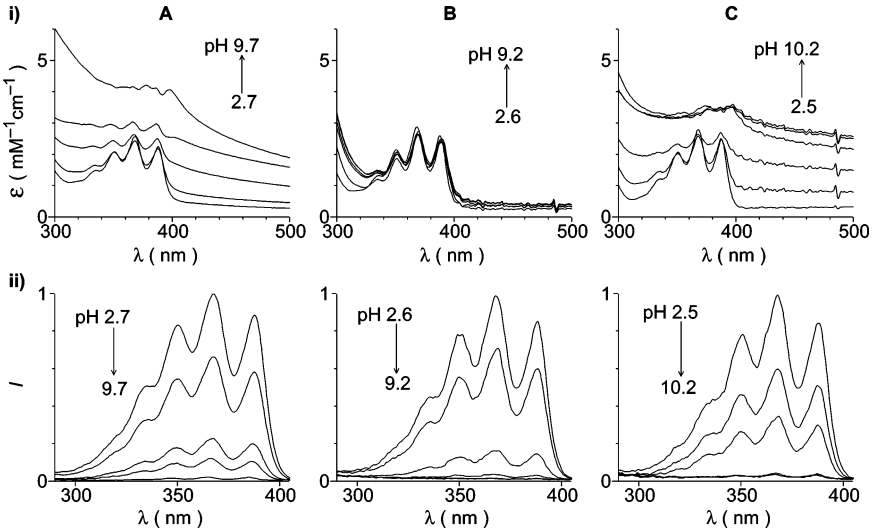


**Figure 2.** pH-dependent change in (i) absorption and (ii) excitation spectra ($\lambda_{em}$ = 416 nm; 298 K) of **L1** in the (A) absence and presence of (B) 1 equiv of $Cu^{2+}$ and (C) 1 equiv of $Zn^{2+}$ in aqueous NaCl or $NaClO_4$ (0.15 M) solution. Changes in absorption and excitation spectra for **L2** are summarized in Figure S2 (see the Supporting Information). The respective spectra in parts i and ii are measured at the following pH values: (A) 2.7, 3.6, 5.7, 7.7, 9.7; (B) 2.6, 3.1, 3.5, 4.1, 6.1, 9.2; and (C) 2.5, 3.4, 4.3, 6.4, 8.3, 10.2.

AN and BP fragments. The lack of red-shifted absorption of **L1** in the presence of $Cu^{2+}$ is because, as reported,[22] the coordinated $Cu^{2+}$ interacts with the $\pi$ electron of the AN moiety in the ground state via a charge transfer, thus suppressing the dipole−dipole interaction between the AN and BP moieties. These facts leave the ENT(AN*→$Cu^{2+}$) process as the main factor for the **L1** fluorescence quenching at pH 4 (Figure 1B.ii). At pH 8, **L1** strongly coordinates with $Cu^{2+}$, which also allows the ELT(AN*→BP) quenching processes as well as the ENT-(AN*→$Cu^{2+}$) process, thus expressing 0 Output. The truth table (Figure 3B) clearly demonstrates that the operation of **L1** by $H^+$ and $Cu^{2+}$ expresses the INHIBIT logic function (Figure 3C).

**3.3. Effect of Other Metal Cations (Expression of the TRANSFER Logic Function).** The most notable feature of the **L1** molecule is that operation by all other metal cations as $Input_2$ expresses the TRANSFER logic function. Figure 5A,B summarizes the results obtained with $Zn^{2+}$ as $Input_2$, for example, a strong AN fluorescence (Output =1) is observed at pH 4 with $Zn^{2+}$ [$Input_1(1)$-$Input_2(1)$], while very weak AN fluorescence is observed at pH 8 with $Zn^{2+}$ [$Input_1(0)$-$Input_2(1)$]. Figure 1C.ii shows the pH-dependent change in the fluorescence intensity of **L1** (open symbols) and **L2** (closed symbols) obtained with 1 equiv of $Zn^{2+}$, where the mole fraction distribution of the different **L1** species (dotted lines) is also shown in this figure, which is calculated from the protonation and stability constants determined potentiometrically (Tables 1 and 2). **L2** shows almost the same distribution of the species as that of **L1**. At pH 4, **L2** scarcely coordinates with $Zn^{2+}$ and, hence, its fluorescence intensity (closed symbols) is almost the same as that obtained without $Zn^{2+}$ (Figure 1A.ii; closed symbols). At pH >4, the intensity of **L2** decreases, because deprotonation of **L2** ($H_2L2^{2+}$ formation) triggers the ELT(N→AN*) quenching process.[13] However, at pH >6, the intensity increases with a $Zn^{2+}$ coordination with **L2**. This is because the $Zn^{2+}$ coordination leads to a decrease in the electron density of the nitrogen atoms and suppresses the ELT(N→AN*) quenching process.[12b,d,21]

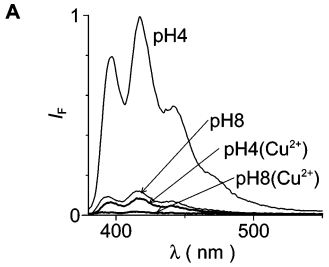


B

| Input$_1$ ($H^+$) | Input$_2$ ($Cu^{2+}$) | Output ($\lambda_{det}$ = 416 nm) |
|---|---|---|
| 0 | 0 | 0 (low, 0.12) |
| 0 | 1 | 0 (low, 0.02) |
| 1 | 0 | 1 (high, 1.00) |
| 1 | 1 | 0 (low, 0.09) |

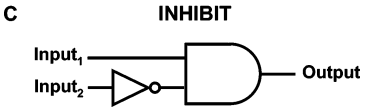


**Figure 3.** (A) Change in fluorescence spectra ($\lambda_{ex}$ = 368 nm; 298 K) of **L1** (40 $\mu$M) in the (normal line) absence and (bold line) presence of 1 equiv of $Cu^{2+}$ in aqueous NaCl (0.15 M) solution at pH 4 or 8, (B) truth table, and (C) INHIBIT logic scheme.

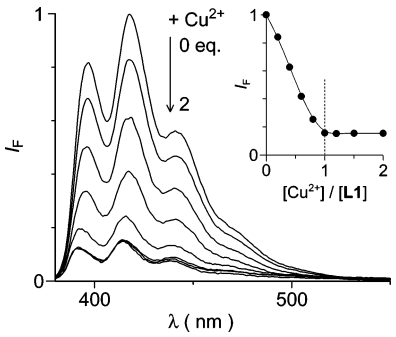


**Figure 4.** Change in fluorescence spectra of **L1** measured at pH 4 as a function of $Cu^{2+}$ amount added ($\lambda_{ex}$ = 368 nm). Inset: Change in the fluorescence intensity (monitored at 416 nm) of **L1** with the $Cu^{2+}$ amount added.

Also in the case for **L1** (Figure 1C.ii, open symbols), addition of $Zn^{2+}$ at pH 4 does not affect the fluorescence intensity. However, at pH >6, **L1** does not show fluorescence enhancement, although **L1** coordinates with $Zn^{2+}$ at this pH: the pH−fluorescence intensity profile is similar to that obtained without $Zn^{2+}$ (Figure 1A.ii, open symbols). $Zn^{2+}$ coordination with **L1** (at pH >4) suppresses the ELT(N→AN*) quenching. However, at the same time, the $Zn^{2+}$ coordination brings the AN and BP fragments closer,[23] which may allow the ELT(AN*→BP) process, thus probably leading to the AN fluorescence quenching. Figure 2C.i shows absorption spectra of **L1** obtained with 1 equiv of $Zn^{2+}$: **L1** with $Zn^{2+}$ shows a red-shifted absorption at pH >4, as is also observed without metal cations (Figure 2A.i).[13] This implies that a dipole−dipole interaction between the AN and BP fragments occurs even with $Zn^{2+}$.[13] In addition, as shown in Figure 6C, $^1$H NMR spectrum of **L1** obtained with $Zn^{2+}$ at pH 8 in a $D_2O/CD_3CN$ (80/20 v/v) solution reveals an upper-field shift of the AN and BP resonances, as compared to the spectrum measured at pH 4 without metal cations (Figure 6A).[12d,13] These findings suggest that the $Zn^{2+}$ coordination actually brings these end fragments closer in the ground state. This means that, at pH 8, the $Zn^{2+}$ coordination with **L1** suppresses the ELT(N→AN*) process but allows the ELT(AN*→BP) process, thus resulting in fluorescence quenching

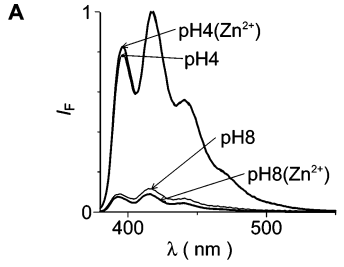


B

| Input$_1$ ($H^+$) | Input$_2$ ($Zn^{2+}$) | Output ($\lambda_{det}$ = 416 nm) |
|---|---|---|
| 0 | 0 | 0 (low, 0.12) |
| 0 | 1 | 0 (low, 0.09) |
| 1 | 0 | 1 (high, 1.00) |
| 1 | 1 | 1 (high, 1.01) |

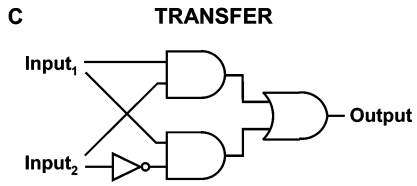


**Figure 5.** (A) Change in fluorescence spectra ($\lambda_{ex}$ = 368 nm; 298 K) of **L1** (40 $\mu$M) in the (normal line) absence and (bold line) presence of 1 equiv of $Zn^{2+}$ in aqueous $NaClO_4$ (0.15 M) solution at pH 4 or 8, (B) truth table, and (C) TRANSFER logic scheme.

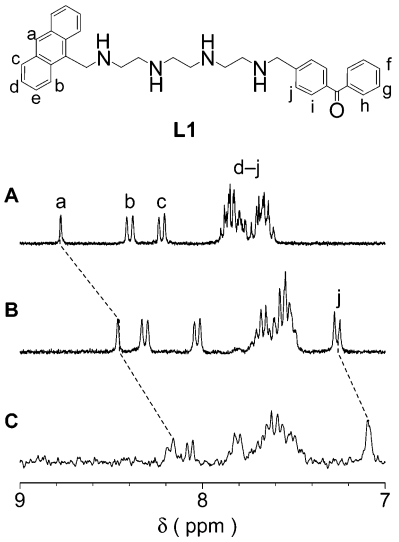


**Figure 6.** $^1$H NMR spectra of **L1** in $D_2O/CD_3CN$ (80/20 *v*/*v*) solution measured (A) at pH 4.0 without metal cations, (B) at pH 8.0 without metal cations, and (C) at pH 8.0 with 1 equiv of $Zn^{2+}$. The pH (= pD − 0.4) of the solutions was adjusted with DCl and NaOD.

(Output = 0).[24] The truth table (Figure 5B) clearly suggests that the operation of **L1** by $H^+$ and $Zn^{2+}$ expresses the TRANSFER logic function (Figure 5C).

Use of all other metal cations ($Ca^{2+}$, $Al^{3+}$, $Eu^{3+}$, $Cd^{2+}$, $Co^{2+}$, $Ni^{2+}$, $Mn^{2+}$, $Hg^{2+}$, and $Pb^{2+}$) except for $Cu^{2+}$, as Input$_2$ also expresses the TRANSFER logic function. As shown in Figure 7, these cations show 1 Output at pH 4, while showing 0 Output at pH 8. In the case of $Ca^{2+}$, $Al^{3+}$, or $Eu^{3+}$, a triethylenetetramine ligand scarcely coordinates with these cations at the entire pH range, as reported,[25] thus showing the same output obtained without metal cations. All other metal cations ($Cd^{2+}$, $Co^{2+}$, $Ni^{2+}$, $Mn^{2+}$, $Hg^{2+}$, and $Pb^{2+}$) can form a complex with a triethylene-

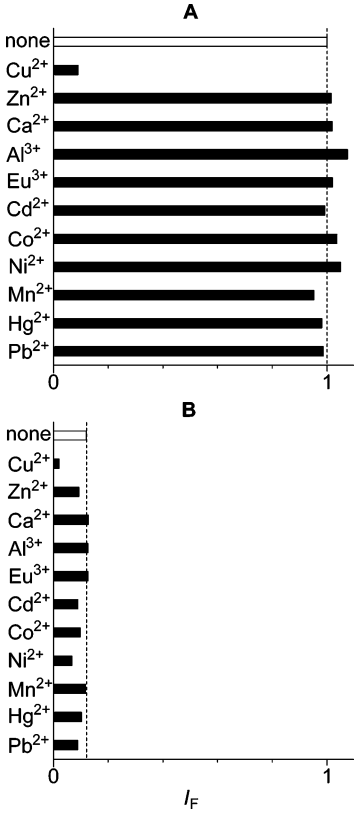


**Figure 7.** Fluorescence intensity of **L1** (40 $\mu$M) measured in aqueous NaCl or $NaClO_4$ (0.15 M) solution at pH (A) 4 and (B) 8 with various metal cations (1 equiv; 40 $\mu$M). The respective fluorescence spectra of **L1** are summarized in Figure S3 (see the Supporting Information).

tetramine ligand, but these show almost the same fluorescence response as that obtained with $Zn^{2+}$ and without metal cations (Figure 7). This is because coordination of **L1** with these metal cations scarcely occurs at pH 4. Table 3 summarizes the conditional stability constants, $K_{cond}$, and free energies, $\Delta G_K$, for coordination between triethylenetetramine (**L**) and various metal cations (1 equiv; $M^{n+}$) at pH 4 and 8, which were determined by the protonation constants and the stability constants for coordination of triethylenetetramine with various metal cations at respective pH,[26] using the following equations:[27]

$$K_{cond} = [M\mathbf{L}]/([M^{n+}]_{free}[\mathbf{L}]_{free}) \quad ([\mathbf{L}]_{free} = \sum[H_n\mathbf{L}]_{free}\ (n = 0-4)) \quad (1)$$

$$\Delta G_K = -RT \log K_{cond} \quad (2)$$

where $R = 8.314$ kJ mol$^{-1}$, $[\mathbf{L}]_{free}$ is the concentration of all of the metal-free diethylenetriamine species at the respective pH, and $T$ is the temperature in Kelvin. The free energies for coordination of triethylenetetramine with all of the metal cations except for $Cu^{2+}$ at pH 4 demonstrate positive $\Delta G_K$ values. This indicates that these metal cations do not coordinate with **L1** at pH 4 and, hence, show the same fluorescence response as that obtained without metal cations (Figure 7A).

In contrast, at pH 8, all these cations show negative $\Delta G_K$ values, indicating that **L1** coordinates with these cations at this pH. The very low fluorescence intensity obtained with the respective cations at pH 8 (Figure 7B) is explained as follows. For $Cd^{2+}$, the coordinated $Cd^{2+}$ suppresses the ELT(N→AN*) quenching process within **L1**, as does $Zn^{2+}$.[12b,d] However, the ELT(AN*→BP) process occurs between the closely situated AN and BP moieties, as is also the case for $Zn^{2+}$, thus leading to the fluorescence quenching (Figure 7B). For $Co^{2+}$, $Ni^{2+}$, or $Mn^{2+}$, coordination of these metal cations with **L1** leads to an energy transfer from the photoexcited AN to their low-lying empty d-orbital [ENT(AN*→metal)],[12d,21] as is also the case for $Cu^{2+}$. In addition, the ELT(AN*→BP) process may also occur between the closely situated AN and BP moieties, thus leading to fluorescence quenching (Figure 7B). Coordination of $Hg^{2+}$ or $Pb^{2+}$, of high atomic number, leads to an enhancement of the intersystem crossing of the photoexcited AN to its nonradiative triplet excited state via a spin−orbital coupling effect[28] as well as the ELT(AN*→BP) process, thus also showing very low fluorescence intensity (Figure 7B). These indicate that the presence of all these metal cations, except for $Cu^{2+}$, does not affect the **L1** fluorescence at both pH 4 and 8, and shows fluorescence outputs just controlled by the presence or absence of $H^+$ (Figure 5), thus resulting in the expression of the TRANSFER logic function.

**TABLE 3: Conditional Stability Constant ($K_{cond}$) and Free Energy ($\Delta G_K$) for Interaction between Triethylenetetramine (L) and Metal Cations ($M^{n+}$) Determined in Water at pH 4 and 8[a]**

| | pH 4 | | pH 8 | |
|---|---|---|---|---|
| $M^{n+}$ | log$K_{cond}$[b] | $\Delta G_K$ (kJ mol$^{-1}$)[c] | log$K_{cond}$[b] | $\Delta G_K$ (kJ mol$^{-1}$)[c] |
| $Cu^{2+}$ | 6.55 | −37.4 | 13.69 | −78.2 |
| $Zn^{2+}$ | −1.51 | 8.6 | 9.30 | −53.0 |
| $Cd^{2+}$ | −2.91 | 16.6 | 7.82 | −44.6 |
| $Co^{2+}$ | −2.59 | 14.8 | 8.00 | −45.7 |
| $Ni^{2+}$ | −1.64 | 9.3 | 11.17 | −63.7 |
| $Mn^{2+}$ | −8.64 | 49.3 | 1.98 | −11.3 |
| $Hg^{2+}$ | −0.60 | 3.4 | 10.28 | −58.7 |
| $Pb^{2+}$ | −1.41 | 8.1 | 8.85 | −50.5 |

[a] $K_w$ (=$[H^+][OH^-]$) value used was $10^{-13.73}$ (ref 15). [b] Calculated by eq 1, where initial concentrations of $[M^{n+}]$ and [**L**] are equal. [c] Calculated by eq 2.

The results presented here reveal that the **L1** molecule acts as a fluorescent molecular logic gate with either−or switchable INHIBIT and TRANSFER logic functions, operated by $H^+$ and metal cation as inputs. These logic functions are easily reconfigured by changing the metal cation inputs. These emission switching functions are driven by the different stability for the metal−**L1** coordination and the resulting photoinduced intramolecular electron and energy transfer processes. The basic concept presented here, which cleverly controls the emission behaviors by a simple-structured molecule, may contribute to the development of more intelligent fluorescent molecular systems.

## 4. Conclusions

Effects of pH and metal cations on the fluorescence behavior of a triethylenetetramine bearing AN and BP fragments, **L1**, have been studied in water. We found that **L1** acts as a fluorescent logic gate with either−or switchable dual logic functions, driven by $H^+$ ($Input_1$) and metal cations ($Input_2$). The results obtained are as follows:

(1) Operation of **L1** at pH 4 (with $H^+$) without metal cations [$Input_1(1)$-$Input_2(0)$] forms monodeprotonated $H_3\mathbf{L1}^{3+}$ species. Within the species, an electron transfer from the photoexcited AN to BP [ELT(AN*→BP)] occurs between the closely situated fragments, while maintaining a strong AN fluorescence (Output = 1). Operation at pH 8 [$Input_1(0)$-$Input_2(0)$] shows very weak fluorescence (Output = 0), where trideprotonated $H\mathbf{L1}^+$ species exist. Within the species, an electron transfer occurs from the nitrogen atoms to the photoexcited AN [ELT(N→AN*)], leading to fluorescence quenching.

(2) Operation of **L1** with $Cu^{2+}$ as $Input_2$ expresses the INHIBIT logic function: **L1** with $Cu^{2+}$ at both pH 4 and 8 [$Input_1(1)$-$Input_2(1)$; $Input_1(0)$-$Input_2(1)$] demonstrates fluorescence quenching (Output = 0). At both conditions, **L1** strongly coordinates with $Cu^{2+}$. This leads to an energy transfer from the photoexcited AN to a low-lying empty d-orbital of the coordinated $Cu^{2+}$ [ENT(AN*→$Cu^{2+}$)], thus resulting in a strong fluorescence quenching.

(3) Operations of **L1** with all other metal cations, except for $Cu^{2+}$, express the TRANSFER logic function. Strong AN fluorescence appears (Output = 1) at pH 4 [$Input_1(1)$-$Input_2(1)$], because **L1** scarcely coordinates with these cations at pH 4. In contrast, fluorescence quenching occurs (Output = 0) at pH 8 [$Input_1(0)$-$Input_2(1)$]. At this pH, the ELT(AN*→BP) process occurs between the AN and BP fragments situated closely by the metal coordination, thus leading to fluorescence quenching.

**Acknowledgment.** This work was partly supported by the Grant-in-Aid for Scientific Research (No. 15360430) and the Grant-in-Aid for Scientific Research on Priority Areas (417) "Fundamental Science and Technology of Photofunctional Interfaces" (No. 17029037) from the Ministry of Education, Culture, Sports, Science and Technology, Japan (MEXT). We are also grateful to the Division of Chemical Engineering for the Lend-Lease Laboratory System. G.N. thanks the Japan Society of Promotion of Science (JSPS) Research Fellowships for Young Scientist.

**Supporting Information Available:** pH-dependent changes in fluorescence (Figure S1) and absorption and excitation (Figure S2) spectra of **L2** in the absence and presence of $Cu^{2+}$ or $Zn^{2+}$; changes in fluorescence spectra of **L1** in the absence and presence of various metal cations (Figure S3); average distance between the AN and BP fragments within metal-free **L1** and Zn**L1**$^{2+}$ species (Table S1). This material is available free of charge via the Internet at http://pubs.acs.org.

## References and Notes

(1) (a) Balzani, V.; Credi, A.; Raymo, F. M.; Stoddart, J. F. *Angew. Chem., Int. Ed.* **2000**, *39*, 3348−3391. (b) de Silva, A. P.; Gunaratne, H. Q. N.; Gunnlaugsson, T.; Huxley, A. J. M.; McCoy, C. P.; Rademacher, J. T.; Rice, T. E. *Chem. Rev.* **1997**, *97*, 1515−1566. (c) Amendola, V.; Fabbrizzi, L.; Mangano, C.; Pallavicini, P. *Acc. Chem. Res.* **2001**, *34*, 488−493.

(2) (a) Drexler, K. E. *Nanosystems*: *Molecular Machinery, Manufacturing and Computation*; Wiley: New York, 1992. (b) Lehn, J.-M. *Supramolecular Chemistry*; VCH: Weinheim, Germany, 1995. (c) de Silva, A. P.; McCoy, C. P. *Chem. Ind.* **1994**, 992−996.

(3) (a) de Silva, A. P.; McClenahan, N. D.; McCoy, C. P. *Molecular-Level Electronics, Imaging and Information, Energy and Environment, in Electron Transfer in Chemistry*; Balzani, V., Ed.; Wiley-VCH: Weinheim, Germany, 2001; Vol. 5. (b) Balzani, V. *Molecular Devices and Machines*: *A Journey into the Nano World*; Wiley-VCH: Weinheim, Germany, 2003. (c) de Silva, A. P.; McClenaghan, N. D. *Chem. Eur. J.* **2004**, *10*, 574−586. (d) Raymo, F. M. *Adv. Mater.* **2002**, *14*, 401−414. (e) Brown, G. J.; de Silva, A. P.; Pagliari, S. *Chem. Commun.* **2002**, 2461−2464.

(4) (a) de Silva, A. P.; Gunaratne, H. Q. N.; McCoy, C. P. *Nature* **1993**, *364*, 42−44. (b) de Silva, A. P.; Gunaratne, H. Q. N.; McCoy, C. P. *J. Am. Chem. Soc.* **1997**, *119*, 7891−7892. (c) de Silva, A. P.; McClean, G. D.; Pagliari, S. *Chem. Commun.* **2003**, 2010−2011. (d) Uchiyama, S.; Kawai, N.; de Silva, A. P.; Iwai, K. *J. Am. Chem. Soc.* **2004**, *126*, 3032−3033. (e) Bag, B.; Bharadwaj, P. K. *Chem. Commun.* **2005**, 513−515.

(5) (a) Ghosh, P.; Bharadwaj, P. K.; Mandal, S.; Ghosh, S. *J. Am. Chem. Soc.* **1996**, *118*, 1553−1554. (b) McSkimming, G.; Tucker, J. H. R.; Bouas-Laurent, H.; Desvergne, J.-P. *Angew. Chem., Int. Ed.* **2000**, *39*, 2167−2169.

(6) (a) de Silva, A. P.; Dixon, I. M.; Gunaratne, H. Q. N.; Gunnlaugsson, T.; Maxwell, P. R. S.; Rice, T. E. *J. Am. Chem. Soc.* **1999**, *121*, 1393−1394. (b) Turfan, B.; Akkaya, E. U. *Org. Lett.* **2002**, *4*, 2857−2859.

(7) (a) Gunnlaugsson, T.; MacDónaill, D. A.; Parker, D. *Chem. Commun.* **2000**, 93−94. (b) Gunnlaugsson, T.; MacDónaill, D. A.; Parker, D. *J. Am. Chem. Soc.* **2001**, *123*, 12866−12867.

(8) Credi, A.; Balzani, V.; Langford, S. J.; Stoddart, J. F. *J. Am. Chem. Soc.* **1997**, *119*, 2679−2681.

(9) Callan, J. F.; de Silva, A. P.; McClenaghan, N. D. *Chem. Commun.* **2004**, 2048−2049.

(10) de Silva, A. P.; Gunnlaugsson, T.; McCoy, C. P. *J. Chem. Educ.* **1997**, *74*, 53−58.

(11) Lee, S. H.; Kim, J. Y.; Kim, S. K.; Lee, J. H.; Kim, J. S. *Tetrahedron* **2004**, *60*, 5171−5176.

(12) (a) Baytekin, H. T.; Akkaya, E. U. *Org. Lett.* **2000**, *2*, 1725−1727. (b) Alves, S.; Pina, F.; Albelda, M. T.; García-España, E.; Soriano, C.; Luis, S. V. *Eur. J. Inorg. Chem.* **2001**, 405−412. (c) de Silva, A. P.; McClenaghan, N. D. *Chem. Eur. J.* **2002**, *8*, 4935−4945. (d) Shiraishi, Y.; Tokitoh, Y.; Hirai, T. *Chem. Commun.* **2005**, 5316−5318.

(13) Nishimura, G.; Shiraishi, Y.; Hirai, T. *Chem. Commun.* **2005**, 5313−5315.

(14) Rodríguez, L.; Alves, S.; Lima, J. C.; Parola, A. J.; Pina, F.; Soriano, C.; Albelda, T.; García-España, E. *J. Photochem. Photobiol. A* **2003**, *159*, 253−258.

(15) Matsuda, K.; Ulrich, G.; Iwamura, H. *J. Chem. Soc., Perkin Trans. 2* **1998**, 1581−1588.

(16) Sabatini, A.; Vacca, A.; Gans, P. *Coord. Chem. Rev.* **1992**, *92*, 389−405.

(17) (a) Shiraishi, Y.; Saito, N.; Hirai, T. *J. Am. Chem. Soc.* **2005**, *127*, 8304−8306. (b) Shiraishi, Y.; Saito, N.; Hirai, T. *J. Am. Chem. Soc.* **2005,** *127*, 12820−12822.

(18) (a) Akkaya, E. U.; Huston, M. E.; Czarnik, A. W. *J. Am. Chem. Soc.* **1990**, *112*, 3590−3593. (b) Shiraishi, Y.; Tokitoh, Y.; Nishimura, G.; Hirai, T. *Org. Lett.* **2005**, *7*, 2611−2614.

(19) Within **L2**, AN and benzene fragments may be brought closer by the deprotonation of the polyamine chain, as is also the case for **L1**. However, ELT(benzene→AN* and AN*→benzene) processes are not favored thermodynamically ($\Delta G_{ELT(benzene\rightarrow AN^*)} = +0.94$ eV.; $\Delta G_{ELT(AN^*\rightarrow benzene)} = +1.34$ eV). **L2** therefore still shows a strong AN fluorescence at pH 2−5 (Figure 1A.ii, closed symbols).

(20) $\tau_N$ is the lifetime of the respective **L1** species due to a natural decay.

(21) (a) Parker, D.; Williams, J. A. G. *J. Chem. Soc., Perkin Trans. 2* **1995**, 1305−1314. (b) Varnes, A. W.; Dodson, R. B.; Wehry, E. L. *J. Am. Chem. Soc.* **1972**, *94*, 946−950. (c) Shiraishi, Y.; Kohno, Y.; Hirai, T. *J. Phys. Chem. B* **2005**, *109*, 19139−19147.

(22) Bernardo, M. A.; Pina, F.; García-España, E.; LaTorre, J.; Luis, S. V.; Llnares, J. M.; Ramírez, J. A.; Soriano, C. *Inorg. Chem.* **1998**, *37*, 3935−3942.

(23) The average distance between the AN and BP fragments within Zn**L1**$^{2+}$ species is determined by semiempirical MO calculation (MNDO-*d* method) to be 9.13 Å. This distance is much smaller than that within metal-free **L1** (21.16 Å) (see the Supporting Information, Table S1).

(24) As shown in Figure 1C.ii (open symbols), the fluorescence intensity of **L1** obtained with $Zn^{2+}$ at pH 4−8 is relatively lower than that obtained without metal cations (Figure 1A.ii, open symbols). As shown in Figure 6C, $^1$H NMR spectra reveal that AN and BP resonances of **L1** measured with $Zn^{2+}$ at pH 8 appear at a field upper than that of **L1** measured at pH 8 without $Zn^{2+}$ (Figure 6B). This indicates that $Zn^{2+}$ coordination brings these end moieties closer than the case without $Zn^{2+}$, and hence accelerates the ELT(AN*→BP) process, resulting in the lower fluorescence intensity.

(25) (a) Poonia, N. S.; Bajaj, A. V. *Chem. Rev.* **1979**, *79*, 389−445. (b) Reilley, C. N.; Schmid, R. W. *J. Elisha Mitchell Sci. Soc.* **1957**, *73*, 279−284.

(26) Martell, A. E.; Smith, R. M. *Critical stability constants*; Plenum Press: New York, 1974; Vol. 2.

(27) (a) Wu, S. L.; Horrocks, W. D., Jr. *Anal. Chem.* **1996**, *68*, 394−401. (b) Aoki, S.; Kaido, S.; Fujioka, H.; Kimura, E. *Inorg. Chem.* **2003**, *42*, 1023−1030. (c) Colette, S.; Amekraz, B.; Madic, C.; Berthon, L.; Cote, G.; Moulin, C. *Inorg. Chem.* **2004**, *43*, 6745−6751.

(28) (a) Vaidya, B.; Zak, J.; Bastiaans, G. J.; Porter, M. D.; Hallman, J. L.; Nabulsi, N. A. R.; Utterback, M. D.; Strzelbicka, B.; Bartsch, R. A. *Anal. Chem.* **1995**, *67*, 4101−4111. (b) Foley, S.; Berberan-Santos, M. N.; Fedorov, A.; Bensasson, R. V.; Leach, S.; Gigante, B. *Chem. Phys.* **2001**, *263*, 437−447.